

Quantum molecular lensing of femtosecond laser optical/plasma filaments^{a)}

S. Varma,^{b)} Y.-H. Chen, and H. M. Milchberg

Institute for Research in Electronics and Applied Physics, University of Maryland, College Park, Maryland 20742, USA

(Received 9 December 2008; accepted 11 December 2008; published online 25 February 2009)

The long-range filamentary propagation of intense femtosecond pulses in atmosphere has been observed for the first time to be strongly effected by quantum rotational wave packets. A two-pulse experiment shows that a filamenting probe pulse can be steered and trapped in or destroyed by the rotational alignment wake following a pump filament. © 2009 American Institute of Physics.

[DOI: [10.1063/1.3078105](https://doi.org/10.1063/1.3078105)]

I. INTRODUCTION

Long-range filamentary propagation of femtosecond pulses in the atmosphere occurs due to the dynamic balance between nonlinear self-focusing of an intense optical pulse and laser plasma-induced defocusing. The effect, which is self-sustaining and can propagate in atmosphere over distances from a few centimeters to hundreds of meters, was first demonstrated in 1995 (Ref. 1) and was subsequently studied by many groups.² Copropagating white light generation and a trailing plasma tail accompany these long-range filaments. The filamentary process can be unstable, and several methods have been proposed to control the formation of single and multiple filaments,^{3,4} which can be used for several applications including remote ionization, broadband light generation and atmospheric monitoring,^{5,6} remote terahertz generation,⁷ and guiding of electrical discharges.⁸ Applications of shorter-range filamentation in gas cells and jets include continuum generation,⁹ high-harmonic generation,¹⁰ and pulse compression.¹¹

This paper presents experimental results showing that the propagation of an intense probe pulse filamenting in air is dramatically affected by the molecular alignment quantum wake following a pump pulse filament. For slight angular pump/probe misalignment, the probe filament is transversely pulled and focused into the pump filament path or destroyed by the wake. The delay between pump and probe pulses, which determines the phase of quantum molecular alignment seen by the probe pulse, determines whether the probe is trapped and focused or destroyed. Although the air nonlinearity for single pulse filamentation is comprised of both a nearly instantaneous response due to bound electronic response and a delayed inertial molecular response, the results confirm that for pulse lengths >100 fs, the rotational component is fast and strong enough to be the overriding effect. Measurements of the spectrum of the probe pulse are consistent with quantum wake trapping. The coherent temporal and spatial response of air molecules can be used to control long-range filamentary propagation of ultrafast optical pulses.

It is well known^{1,2} that filament formation and propaga-

tion is the effect of interplay between the third-order nonlinearity and ionization. The critical power in air for self-focusing and the onset of filament formation for femtosecond pulses is typically observed to be $P_{cr} \sim 5-10$ GW.^{1,2} This value is higher than ~ 1.8 GW predicted by previous long pulse measurements of the nonlinear index n_2 ,¹² where $P_{cr} = 3.77\lambda^2/8\pi n_0 n_2$. This issue is discussed in detail later.

Once the self-focused intensity is high enough, plasma begins to be generated along the beam axis by means of multiphoton and field ionization of gas atoms or molecules. The free electrons form a negative lens that arrests self-focusing and causes refractive beam divergence. The third-order nonlinearity eventually causes sufficient nonlinear phase to accumulate, and then self-focusing and plasma-induced divergence repeat. In this way, both the laser intensity and the plasma density are limited to maximum values—the laser intensity in air is clamped at $\sim 5 \times 10^{13}$ W/cm² (Ref. 2) and the gas ionization fraction at $\sim 10^{-4}-10^{-3}$.^{2,13} These experimental measurements have been confirmed by simulations.¹⁴ Over the course of many meters of propagation, the plasma filament can retain a diameter of tens of microns.¹⁵

II. ROTATIONAL WAVE PACKET EXCITATION IN ATMOSPHERIC CONSTITUENTS

Nitrogen and oxygen are linear molecules that rotate in intense laser fields due to the fact that their induced dipole moments depend on the orientation of their molecular axes with respect to the laser polarization. Consequentially, randomly aligned N₂ and O₂ molecules experience a net torque in an intense laser field toward alignment with the field.¹⁶ This effect is significant in molecular ensembles at room temperature up to multiple atmospheres of pressure

The molecular alignment by the electric field can be expressed as the excitation of a quantum-mechanical wave packet $|\psi\rangle = \sum_{j,m} a_{j,m} |j,m\rangle e^{-i\omega_j t}$ of rotational states $|j,m\rangle$ of energy $E_{j,m} = \hbar\omega_j = hcBj(j+1)$, where j is the quantum number for total rotational angular momentum, m is the momentum component along the laser field, h is Planck's constant, and B is the rotational constant of the molecule.¹⁶ Because m is the quantum number for the component of angular momentum along the laser field, it does not change. In Raman

^{a)}Paper N12, 6, Bull. Am. Phys. Soc. 53, 163 (2008).

^{b)}Invited speaker.

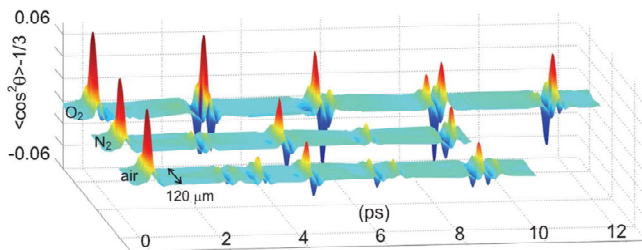


FIG. 1. (Color online) Measured alignment of 1 atm of N_2 and O_2 at room temperature (295 K) by a 110 fs, 800 nm, 4.1×10^{13} W/cm² laser pulse. The effective alignment of air is synthesized from the N_2 and O_2 plots.

terminology, one photon excites the molecule to a virtual state which is then stimulated downward to an excited rotational level by a slightly redder photon within the laser bandwidth. Because the femtosecond laser pulse is much shorter than the molecular rotation period, it phase locks the rotational modes, which results in a coherent initial molecular alignment and sharp recurrences of the alignment well after the pump pulse. These alignment revivals are analogous to the train of short optical pulses (mode-locked pulses) that result from phase-locked longitudinal modes of an optical cavity. The molecular alignment recurrences occur dominantly at dominantly at $\frac{1}{4}T, \frac{1}{2}T, \frac{3}{4}T, T, \frac{5}{4}T, \dots$, where $T = 1/2Bc$ is the rotational period.¹⁷ The full revival period of N_2 gas is $T_{N_2} = 8.3$ ps, while $T_{O_2} = 11.6$ ps.¹⁸

The alignment recurrences have a transient effect on the index of refraction in the focal volume of the laser beam. The refractive index transients can be measured by a weak probe beam^{9,18–20} and the intensity and phase modulation imprinted on the probe pulse have been used to impart spectral and temporal modulation.^{9,21,22}

Figure 1 shows the alignment revivals induced by a 100 fs pump pulse in a gas cell filled with pure nitrogen or oxygen. The revivals were measured in space and in time with 10 fs resolution using single-shot supercontinuum spectral interferometry.⁹ The time-dependent molecular alignment is represented as $\langle \cos^2 \theta \rangle_{t-1/3}$, where θ is the angle between the laser polarization and the molecular axis,⁹ $\langle \rangle_t$ is the time-dependent ensemble average, and $\frac{1}{3}$ is the average alignment of a randomly oriented molecule. For a pure molecular gas, the refractive index shift $\Delta n(r, t)$ owing to the alignment experienced by a parallel polarized probe pulse is given by⁹ $\Delta n(r, t) = 2\pi N n_0^{-1} \Delta \alpha_{N_2} (\langle \cos^2 \theta \rangle_{t-1/3})$, where r is the coordinate transverse to the beam, N is the molecular density, $\Delta \alpha = \alpha_{\parallel} - \alpha_{\perp}$ [where α_{\perp} and α_{\parallel} are the linear polarizabilities along the short and long molecular axes, $\Delta \alpha_{N_2} = 0.93 \times 10^{-24}$ cm³, and $\Delta \alpha_{O_2} = 1.14 \times 10^{-24}$ cm³ (Ref. 18)], and $n_0 \sim 1$ is the isotropic refractive index before the pump arrives. Figure 1 also shows the effective alignment response of air, synthesized by using the approximate atmospheric fractional abundances of N_2 (80%) and O_2 (20%) in the expression $\Delta \alpha_{\text{eff}} = 0.8 \Delta \alpha_{N_2} + 0.2 \Delta \alpha_{O_2}$ and forming $\langle \cos^2 \theta \rangle_{t, \text{eff}} = 0.8 (\Delta \alpha_{N_2} / \Delta \alpha_{\text{eff}}) \langle \cos^2 \theta \rangle_{t, N_2} + 0.2 (\Delta \alpha_{O_2} / \Delta \alpha_{\text{eff}}) \langle \cos^2 \theta \rangle_{t, O_2}$. In our experiments, we use a probe pulse perpendicularly polarized to the pump pulse in order to differentiate between the two and extract the effect on the probe of the molecular

alignment by the pump. In this case, we replace $\langle \cos^2 \theta \rangle_t$ with $\frac{1}{2}(1 - \langle \cos^2 \theta \rangle_t)$.

The difference in phase between the center and waist of a Gaussian beam a Rayleigh length (z_0) after focus is of order unity. Over the same distance, an on-axis refractive index bump Δn would retard the phase of the center of the beam by $k \Delta n z_0$, where k is the vacuum wave number. A fractional increase in the index of refraction at the center of a beam Δn will compete with beam diffraction if $\Delta n > (k z_0)^{-1}$. Therefore, a laser beam launched with f number $f_{\#} = \frac{1}{2}(\pi z_0 / \lambda)^{1/2} > \frac{1}{2}(2 \Delta n)^{-1/2} = f_{\#, \text{molec}}$ should be significantly affected by atmospheric molecular alignment revivals, where $f_{\#, \text{molec}}$ is an effective f number due to Δn from alignment. For example, at the peak of the air quantum revival near $t = 8$ ps, which is comprised of the full revival of N_2 and the $\frac{3}{4}$ revival of O_2 , $\langle \cos^2 \theta \rangle_{t, \text{eff}} - \frac{1}{3} \sim 0.025$, giving $\Delta n(r=0) \sim 3 \times 10^{-6}$ at atmospheric pressure, and giving $f_{\#, \text{molec}} \sim 200$. A molecular effect on propagation then requires $f_{\#} > 200$.

The dominant ultrafast contribution of rotational quantum wave packets for ultrashort laser pulses ~ 40 fs or longer is often overlooked. A wave packet is a coherent sum of rotational states up to the maximum rotational quantum number j_{max} . At room temperature and $I \sim 4 \times 10^{13}$ W/cm², $j_{\text{max}} \sim 20$. The refractive index response time due to the alignment effects of such a wave packet is $\delta t \sim 2T / j_{\text{max}}(j_{\text{max}} + 1)$,⁹ giving $\delta t \sim 40$ fs. This time scale is confirmed by the inset of Fig. 3(a), which shows a center lineout of the air response from Fig. 1. Molecular alignment dominates the nonlinear response of air unless a pulse is appreciably shorter than δt , in contrast to earlier work,²³ in which the relative rotational and isotropic contributions for 100 fs pulses were taken to be equal. The nonlinear index of refraction obtained from the inset gives $P_{\text{cr}} = 10$ GW at the laser pulse peak and $P_{\text{cr}} = 4.3$ GW at the molecular response peak.

III. EXPERIMENTAL SETUP

The experimental setup is shown in Fig. 2. A dual polarization interferometer (DPI) is used to produce two orthogonally polarized pulses with tunable energy from a single input pulse. The delay between the two pulses is adjusted using a computer controlled stepper motor on the retroreflecting arm. The alignment of the two arms of the DPI can be individually tuned for collinear propagation, though in some experiments the two pulses were deliberately angularly separated. The two pulses, each 800 nm, 130 fs, and with a few millijoules of energy, are apertured to 1 cm diameter and focused by a 3 m lens at $f_{\#, \text{lens}} \sim 300$. The dual pulse beam then propagates 6 m across the laboratory and enters a filament profile imaging system (not pictured). This system uses two glass wedges to attenuate the beam intensity, a cube polarizer to remove the pump pulse, and a lens which images the probe filament onto a charge coupled device camera. The filament is typically > 2 m long and the imaging system images a plane 25 cm after the end of the filament. Figure 2 also shows a sequence of single beam images on a far-field screen, taken by a digital camera. These images show the

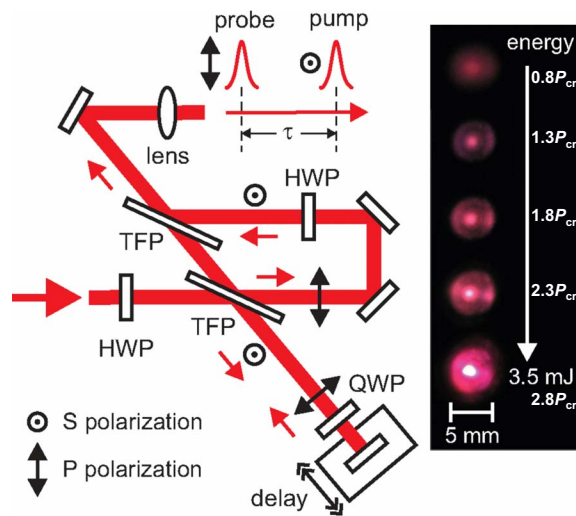


FIG. 2. (Color online) Setup showing the DPI. QWP=quarter-wave-plate; HWP=half-wave-plate; TFP=thin film polarizer. The right panel shows beam images of filamentation and white light generation for increasing pulse power up to $\sim 2.8P_{cr}$.

onset of filamentation and white light generation up to $2.8P_{cr}$ (using $P_{cr}=10$ GW).

IV. RESULTS AND DISCUSSION

The strong effect of molecular alignment on the filamentary propagation of the probe pulse is first demonstrated by an experiment in which the probe pulse copropagates with the pump pulse at delays near $t \sim 0$, where the pump and probe can be temporally overlapped. The vertically polarized pump pulse (1.4 mJ, $1.1P_{cr}$) generates a filament which is preceded or followed by the horizontally polarized probe filament (2 mJ, $1.5P_{cr}$). The results are shown in Fig. 3(a), where slices of the image of the probe filament are plotted versus delay. Thirty images were taken at each 30 fs intervals, averaged and converted into slices by integrating the two-dimensional (2D) profiles along their vertical axis. Sample 2D images are shown at several delays. A strong probe pulse filament is seen, as expected, well before $t=0$, but within approximately 50 fs of overlap, the probe filament is extinguished [location A in Fig. 3(a)] and remain so until ~ 50 fs beyond overlap, at which point the strong probe filament returns. This is proof that ionization-induced defocusing is not the cause of probe filament destruction, since the filament recovers in ~ 100 fs, whereas the plasma lifetime is many nanoseconds.¹³ The temporary destruction is a direct result of the orientational contribution to the nonlinearity of the neutral gas. If the probe was polarized parallel to the pump, the molecular alignment from the pump would focus the probe near $t=0$. However, in this experiment, the probe is perpendicularly polarized and would defocus. The ~ 100 fs interval over which the probe filament is destroyed is consistent with the molecular defocusing interval. Figure 3(b) repeats the format of Fig. 3(a) for 330 fs pulses with pump/probe energies of 5.85 mJ/7.25 mJ ($3.7P_{cr}/4.6P_{cr}$) using 85 fs delay steps. The probe filament disruption interval is slightly broader, which is expected due to the longer pump pulse.

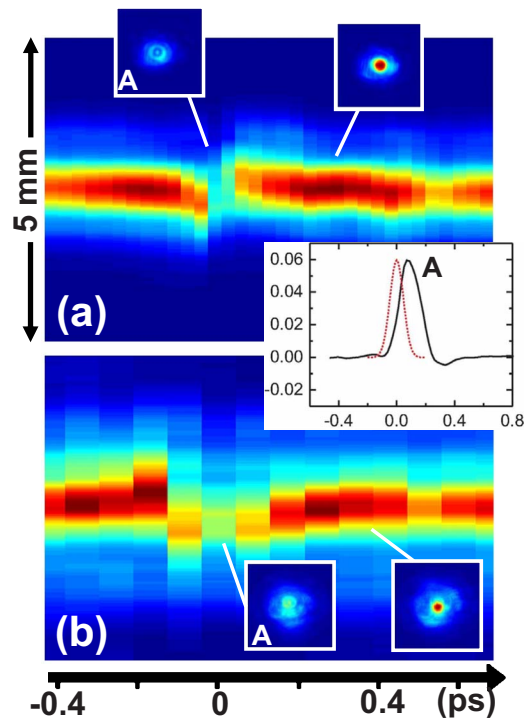


FIG. 3. (Color online) (a) One-dimensional (1D) integrated images of the probe filament as a function of delay (30 fs steps) through the pump-probe temporal overlap ($t=0$). The laser pulse width is 130 fs. Pump/probe energies are 1.4 mJ/2 mJ ($1.1P_{cr}/1.6P_{cr}$). Each image slice is a 30-shot average. Selected 2D images are shown as insets, as is a beam center lineout of the air alignment response (black line) and the pump pulse (red squares) in the $t=0$ region. (b) Scan as in (a) but with 330 fs laser pulses, 85 fs delay steps, and pump/probe energies of 5.85 mJ/7.25 mJ ($3.7P_{cr}/4.6P_{cr}$).

The effect of the pump filament rotational wave packet excitation on the probe filament can be decoupled from the pump pulse's bound electronic effect by examining the probe filament at delays much later than $t=0$ that coincide with recurrences of the molecular alignment. Figure 4(a) shows results near $t=8$ ps, near which the probe pulse experiences the summed effects of the full revival of N_2 and the $\frac{3}{4}$ revival of O_2 . The pump/probe energies are 1.4 mJ ($1.1P_{cr}$)/2.5 mJ

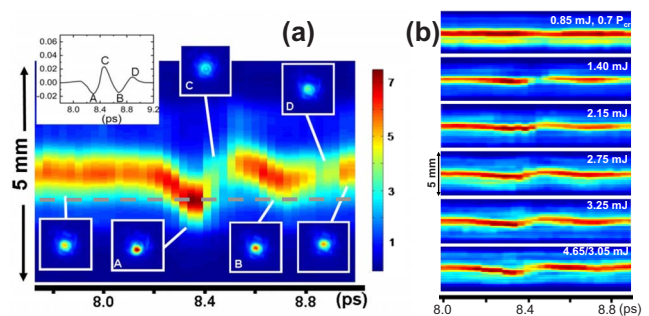


FIG. 4. (Color online) (a) 1D integrated images of probe filament as a function of delay (30 fs steps) through the air revival near $t=8$ ps, comprised of the N_2 full revival ($t \sim T_{N_2} \sim 8.3$ ps) and the O_2 three-quarter revival ($t = \frac{3}{4}T_{O_2} \sim 8.7$ ps). Pump/probe energies are 1.4 mJ/2.5 mJ ($1.1P_{cr}/2.5P_{cr}$). The gray dashed line shows the position of the center of the pump filament. Selected 2D images are shown as insets, as is a lineout of the air alignment response in the $t=8$ ps region. (b) Pump pulse energy scan ($0.7P_{cr}$ to $2.5P_{cr}$), holding probe energy constant at 4.35 mJ ($3.4P_{cr}$). The bottom panel has pump/probe energies of 4.65 mJ/3.05 mJ ($3.6P_{cr}/2.4P_{cr}$).

($1.9P_{cr}$), and the two pulses are angularly separated by ~ 0.1 mrad. The gray dashed line shows the transverse position of the center of the pump filament, and therefore also highlights the regions of maximally aligned air molecules. Here we see, depending on delay, that the probe filament can not only be extinguished but it can be trapped and enhanced. The inset in Fig. 4(a) shows the molecular alignment near $t = 8$ ps. From this, it is clear that the temporal evolution of the molecular alignment maps exactly onto the focusing and defocusing intervals of the probe filament. The delays at which the probe is steered into the pump beam path and enhanced (labeled A and B in the figure) correspond precisely with anti-alignment peaks in the inset. The inset shows alignment as it would be seen by a parallel polarized probe, so for the perpendicularly polarized probe experiment, as expected, we see the opposite effect. The filament destruction at locations C and D are coincident with molecular alignment. The probe filament returns to its original position after the revival. Full images of the probe filament at selected delays are shown as additional insets. Depending on pump-probe alignment and on a shot-by-shot basis, the probe filament “destruction” is seen as either wild swings of the filament position or as filament breakup. The steering effect on the probe filament is analyzed by examining off-axis Δn from molecular alignment. Trapping can occur if $k\Delta nL \sim 1$, where L is the filament length and is approximately 2 m. The off-peak Δn required for trapping is then $\sim 6 \times 10^{-8}$ (0.002 of the measured Δn_{peak} value at $r=0$). If the pump and probe are misaligned by 0.1 mrad at their source, the DPI, they are separated by $\sim 350 \mu\text{m}$ at the onset of filamentation. If the molecular lens profile corresponds to a filament full width at half maximum diameter of $\sim 100 \mu\text{m}$ diameter, then $\Delta n/\Delta n_{peak} \sim 0.002$ at $r \sim 200 \mu\text{m}$, and the probe filament will have some spatial overlap with enough molecular alignment to be steered and trapped in the wake of the pump pulse.

Figure 4(b) shows the result from a repeat of the delay scan of the probe pulse near $t = 8$ ps seen in Fig. 4(a), with the probe energy fixed (4.4 mJ, $3.4P_{cr}$) and varying pump energy. At the lowest pump energy (0.85 mJ, $0.7P_{cr}$), the molecular effect is not evident. This is reasonable, since a nonfilamenting pump pulse will only be intense enough to significantly align air molecules over its Rayleigh range, which is ~ 10 cm and much shorter than the filament length. Notably, as the pump energy is increased to values greater than that of the probe, the steering, enhancement, and destruction of the probe filament remain evident. The visible robustness of the molecular effect over such a wide range of pump and probe powers is discussed below.

Figure 5 again shows the probe filament profile near $t = 8$ ps but in the case where the pump pulse (3.6 mJ, $2.8P_{cr}$) and the probe (4.6 mJ, $3.6P_{cr}$) are not misaligned. The significant aspect of these data is the reservoir² of laser energy surrounding the filament. It is evident that the enhancement [labeled A in the data and corresponding to the Fig. 4(a) inset] of the probe filament comes at the expense of the reservoir. Conversely, molecular anti-alignment (labeled C) clearly expels light into the reservoir.

Figure 6 shows the result of a second experiment, where

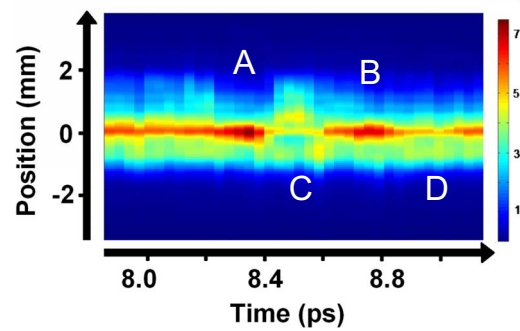


FIG. 5. (Color online) As in Fig. 4(a), 1D integrated images of the probe filament as a function of delay near $t = 8$ ps but with no pump/probe misalignment. Pump/probe energies are 3.6 mJ/4.6 mJ ($2.8P_{cr}/3.6P_{cr}$). Note the funneling of laser energy from the reservoir into the filament at location A and the expulsion of filament light at location B.

we copropagate two 130 fs pulses with the same polarization. This is done by inserting a Mach-Zehnder interferometer between the stretcher and the regenerative amplifier of the Ti:sapphire chirped-pulse amplification (CPA) system. The system output is two perfectly collinear pulses, each 3.3 mJ ($2.6P_{cr}$) with adjustable delay. Due to their parallel polarization, the pump cannot be passively filtered to extract the probe response. However, the pump filament little affects the probe filament beam profile at delays detuned from the molecular alignment revivals, so a combined image of pump and probe can be taken at one of these delays and halved in intensity to construct the image of the pump alone. This can then be subtracted from all combined pump-probe images to yield the probe image. The effective molecular alignment seen by the probe pulse in this case should be double that from the first experiment, because alignment is symmetric only around the input pulse polarization. In the first experiment, the “aligned” molecules are actually equally likely to be oriented in the horizontal direction and the direction of propagation. The enhancement effect at position A is greater than that from the experiment with perpendicularly polarized filaments, although shot to shot laser fluctuations prevented observation of a stronger enhancement.

White light generation is a feature of filamentation that is also enhanced when the probe filament is trapped in a quantum molecular wake. This effect is demonstrated in Fig.

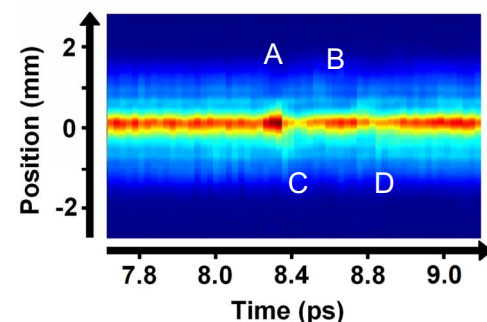


FIG. 6. (Color online) 1D integrated images of the probe filament aligned with a parallel polarized pump filament as a function of delay near $t = 8$ ps. The pump and probe are perfectly collinear and each have energy of 3.3 mJ ($2.6P_{cr}$).

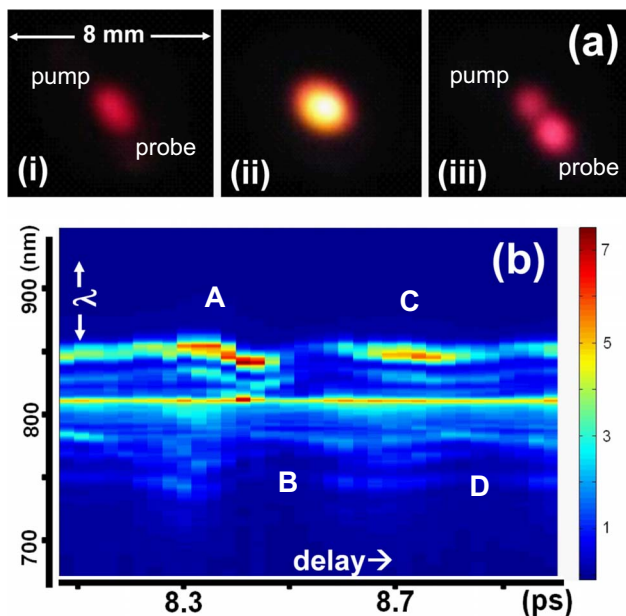


FIG. 7. (Color online) (a) Pump ($2.3P_{cr}$) and probe ($2.5P_{cr}$) filament central spots in far field with initial ~ 0.1 mrad misalignment, where (i) probe delay is detuned from revivals, (ii) probe is delayed to location A in Fig. 4(a), and (iii) probe is delayed to location C in Fig. 4(a). (b) Probe filament spectrum as a function of delay (33 fs steps) through the air alignment revival near $t=8$ ps.

7(a), a series of three single-shot, far-field photographs of the pump ($2.3P_{cr}$) and probe ($2.5P_{cr}$) pulses on a screen. Panel (i) shows the pump and probe filament spots offset by ~ 0.1 mrad with the probe delay detuned from any revivals. In panel (ii), when the probe delay is tuned to position C from Fig. 4(a), it is steered into the alignment wake of the pump filament and trapped. Here, there is a great increase in generated white light, confirming higher probe intensity and suggesting an increase in the length of the probe filament. Panel (iii) shows the probe filament delayed to the anti-aligned molecules at position A from the same figure. The negative-lensing effect is so strong that the probe filament is clearly expelled away from the pump.

A spectrometer was placed after the cube polarizer to examine the probe filament spectrum as a function of delay near $t=8$ ps. The results are plotted in Fig. 7(b). Though spectra and phase have been measured for weak optical pulses that probe rotational wakes in gas cells,^{9,20–22} this is the first measurement of the spectrum of a high power filament which probes such wakes in atmosphere. Generally, broadening and narrowing of the filament spectrum are evident at, respectively, the focusing and defocusing intervals of molecular alignment. The narrowing is simply explained by the destruction of the filament over these intervals; the less intense a filament is or the shorter distance it persists, the less nonlinear phase can be accrued. Part of the broadened blue wing of the spectrum is explained by molecular focusing causing extra ionization at positions A and B in Fig. 4(a), leading to $\Delta\omega_{lin} > 0$ from ionization self-phase modulation. The rest of the broadening and the finer features of the spectral modulation versus delay can also be qualitatively explained by understanding that the quantum molecular revival

is a time-dependent refractive index shift and therefore contributes phase modulation in the form of linear and quadratic frequency shifts: $\Delta\omega_{lin} \sim -\partial\Phi/\partial t$ and $\Delta\omega_{quad} \sim -(t-t_0) \times (\partial^2\Phi/\partial t^2)_{t=t_0}$, where $t=t_0$ is the peak of the local alignment at a point such as location A in Fig. 4(a). The probe pulse propagating alongside the revival in the vicinity of this delay will experience both $\Delta\omega_{lin}$ and $\Delta\omega_{quad}$. If the probe is positioned at the alignment inflection points, the revival temporal profile gives both positive and negative $\Delta\omega_{lin}$. When the probe pulse is nestled precisely in the alignment waveform at intervals A or B, it experiences $\partial^2\Phi/\partial t^2 > 0$, which explains the redshift (for $t > t_0$) following the blueshift (for $t < t_0$) at A and B.

To complete the physical picture of the molecular effect on filament propagation, we must also consider plasma generation. The lens and molecular alignment focusing effects are additive, so $f_{\#,lens} \sim 300$ and $f_{\#,molec} \sim 200$ combine to give $f_{\#,eff}^{-1} = f_{\#,lens}^{-1} + f_{\#,molec}^{-1} \sim 1/120$. Plasma-induced beam defocusing only competes with molecular and lens focusing for $\frac{1}{2}(\Delta n_{plasma})^{-1/2} > f_{\#,eff}$, where $\Delta n_{plasma} = N_e/2N_{cr}$, N_e is the electron density, and $N_{cr} \sim 1.7 \times 10^{21} \text{ cm}^{-3}$ is the critical density for an 800 nm wavelength. For our $f_{\#,eff}$, $N_e/N_{cr} < 1.7 \times 10^{-5}$. This is a fractional ionization of $< 10^{-3}$ at atmospheric pressure, consistent with earlier measurements.^{2,13} So even at the highest laser powers, essentially all molecules survive, explaining the robustness of the molecular effect.

V. SUMMARY

We have demonstrated that ultrafast rotational quantum wave packet excitation of N_2 and O_2 significantly affects the long-range filamentary propagation of a femtosecond optical pulse in atmosphere. The initial alignment of air molecules is prompt enough to dominate the nonlinear response and filamentation of pulses with duration $> \sim 100$ fs. Additionally, the molecular alignment revivals following a pump filament persist over long time durations, are robust over a wide range of pulse energies, and can be effectively used to manipulate the intensity, position, and spectral content of an intense probe filament. The enhancement of the probe filament intensity may result in an increase in filament length and electron density.

ACKNOWLEDGMENTS

This work was supported by the National Science Foundation, the U.S. Department of Energy, and the Johns Hopkins Applied Physics Laboratory.

¹A. Braun, G. Korn, X. Liu, D. Du, J. Squier, and G. Mourou, *Opt. Lett.* **20**, 73 (1995).

²A. Couairon and A. Mysyrowicz, *Phys. Rep.* **441**, 47 (2007) and references therein.

³S. Eisenmann, E. Louzon, Y. Katzir, T. Palchan, A. Zigler, Y. Sivan, and G. Fibich, *Opt. Express* **15**, 2779 (2007); G. Fibich, Y. Sivan, Y. Ehrlich, E. Louzon, M. Fraenkel, S. Eisenmann, Y. Katzir, and A. Zigler, *ibid.* **14**, 4946 (2006).

⁴S. Varma, Y.-H. Chen, and H. M. Milchberg, *Phys. Rev. Lett.* **101**, 205001 (2008).

⁵I. Alexeev, A. C. Ting, D. F. Gordon, E. Briscoe, B. Hafizi, and P. Sprangle, *Opt. Lett.* **30**, 1503 (2005).

- ⁶J. Kasparian, M. Rodriguez, G. Méjean, J. Yu, E. Salmon, H. Wille, R. Bourayou, S. Frey, Y.-B. André, A. Mysyrowicz, R. Sauerbrey, J.-P. Wolf, and L. Wöste, *Science* **301**, 61 (2003).
- ⁷C. D'Amico, A. Houard, M. Franco, B. Prade, and A. Mysyrowicz, A. Couairon, and V. Tikhonchuk, *Phys. Rev. Lett.* **98**, 235002 (2007); Y. Liu, A. Houard, B. Prade, S. Akturk, A. Mysyrowicz, and V. T. Tikhonchuk, *ibid.* **99**, 135002 (2007).
- ⁸R. P. Fischer, A. C. Ting, D. F. Gordon, R. F. Fernsler, G. P. DiComo, and P. Sprangle, *IEEE Trans. Plasma Sci.* **35**, 1430 (2007); A. Houard, C. D'Amico, Y. Liu, Y. B. Andre, M. Franco, B. Prade, A. Mysyrowicz, E. Salmon, P. Pierlot, and L.-M. Cleon, *Appl. Phys. Lett.* **90**, 171501 (2007).
- ⁹Y.-H. Chen, S. Varma, A. York, and H. M. Milchberg, *Opt. Express* **15**, 11341 (2007); Y.-H. Chen, S. Varma, I. Alexeev, and H. M. Milchberg, *ibid.* **15**, 7458 (2007).
- ¹⁰H. R. Lange, A. Chiron, J.-F. Ripoché, A. Mysyrowicz, P. Breger, and P. Agostini, *Phys. Rev. Lett.* **81**, 1611 (1998); Y. Tamaki, J. Itatani, Y. Nagata, M. Obara, and K. Midorikawa, *ibid.* **82**, 1422 (1999).
- ¹¹C. P. Hauri, W. Kornelis, F. W. Helbing, A. Heinrich, A. Couairon, A. Mysyrowicz, J. Biegert, and U. Keller, *Appl. Phys. B: Lasers Opt.* **79**, 673 (2004).
- ¹²Y. Shimoji, A. T. Fay, R. S. F. Chang, and N. Djeu, *J. Opt. Soc. Am. B* **6**, 1994 (1989); D. M. Pennington, M. A. Henesian, and R. W. Hellwarth, *Phys. Rev. A* **39**, 3003 (1989).
- ¹³S. Eisenmann, A. Pukhov, and A. Zigler, *Phys. Rev. Lett.* **98**, 155002 (2007).
- ¹⁴P. Sprangle, J. R. Peñano, and B. Hafizi, *Phys. Rev. E* **66**, 046418 (2002).
- ¹⁵A. Ting, D. F. Gordon, E. Briscoe, J. R. Peñano, and P. Sprangle, *Appl. Opt.* **44**, 1474 (2005).
- ¹⁶H. Stapelfeldt and T. Seideman, *Rev. Mod. Phys.* **75**, 543 (2003).
- ¹⁷P. W. Dooley, I. V. Litvinyuk, K. F. Lee, D. M. Rayner, M. Spanner, D. M. Villeneuve, and P. B. Corkum, *Phys. Rev. A* **68**, 023406 (2003).
- ¹⁸C. H. Lin, J. P. Heritage, T. K. Gustafson, R. Y. Chiao, and J. P. McTague, *Phys. Rev. A* **13**, 813 (1976).
- ¹⁹V. Renard, O. Faucher, and B. Lavorel, *Opt. Lett.* **30**, 70 (2005).
- ²⁰J.-F. Ripoché, G. Grillon, B. Prade, M. Franco, E. Nibbering, R. Lange, and A. Mysyrowicz, *Opt. Commun.* **135**, 310 (1997).
- ²¹R. A. Bartels, T. C. Weinacht, N. Wagner, M. Baertschy, C. H. Greene, M. M. Murnane, and H. C. Kapteyn, *Phys. Rev. Lett.* **88**, 013903 (2001).
- ²²F. Calegari, C. Vozzi, S. Gasilov, E. Benedetti, G. Sansone, M. Nisoli, S. De Silvestri, and S. Stagira, *Phys. Rev. Lett.* **100**, 123006 (2008).
- ²³E. T. J. Nibbering, G. Grillon, M. A. Franco, B. S. Prade, and A. Mysyrowicz, *J. Opt. Soc. Am. B* **14**, 650 (1997).